Eur. Phys. J. B (2016) 89: 101
DOI: 10.1140/epjb/e2016-60949-1

THE EUROPEAN PHYSICAL JOURNAL B

Regular Article

# On the possibility that local mechanical forcing permits directionally-controlled long-range electron transfer along DNA-like molecular wires with no need of an external electric field

## Mechanical control of electrons

Alexander P. Chetverikov[1], Werner Ebeling[2], Viktor D. Lakhno[3], Alexey S. Shigaev[3], and Manuel G. Velarde[4,a]

[1] Deptartement of Physics, Saratov State University, Astrakhanskaya 83, 410012 Saratov, Russia
[2] Institut für Physik, Humboldt Universität Berlin, Newtonstrasse 15, 12489 Berlin, Germany
[3] Institute of Mathematical Problems of Biology, Russian Academy of Sciences, Institutskaya 4, 142290 Puschino, Russia
[4] Instituto Pluridisciplinar, Universidad Complutense, Paseo Juan XXIII, 1, 28040 Madrid, Spain

Received 10 December 2015
Published online 18 April 2016 – 

**Abstract.** It is shown that in DNA-like molecules containing added, excess charges, such as electrons and holes (cation-radicals), it is possible by highly energetic, local, mechanical excitation at definite places of the chain to control the creation of breathers/bubbles and hence to control the long-range transfer of charges moving along the chain in a definite given direction with no external electric field needed.

## 1 Introduction

The study of physicochemical properties, local fluctuations of DNA structure and charge transfer in this polymer molecule is of great interest for molecular biology and biophysics [1–7], as well as for the relatively new science of nanobioelectronics [8,9]. The DNA molecule is a polymer consisting of two chains which usually form a right-handed double helix – $\alpha$-duplex. The spatial structure of $\alpha$-duplex is provided by hydrogen bonds (H-bonds) joining nitrogenous bases of different chains and by partial delocalization of $\pi$-electrons between neighboring bases of one chain. Today there are possibilities to manipulate not only the sequence of nucleotides but also to create locally excitations such as oscillations, kinks, etc. Here we show how to control properties of DNA open state like bubbles and some processes such as long-range electron transfer (ET) by local excitations.

The critical temperature, local stability, electric conductivity and other properties of a DNA duplex depend greatly on its primary structure, i.e., a linear sequence of bases, see for example [10–16]. In the study of DNA properties simple mathematical models in which each base pair is described by a small number of properties are useful to study the processes of mechanical excitations leading to energy transfer. The energy localization leads to local destabilization of the DNA structure and emergence of localized openings of DNA duplex, i.e., local unwinding of its chains [10]. This property was often used to explain the results of experiments on DNA with different nucleotide sequences [14,15,17,18]. We will show here for a rather simple model that it is possible to control the creation of breathers/bubbles and polarons by local excitations generated from outside. Further we will show that the moving of excess charges on the lattice can be influenced and controlled. In order to control the creation and the direction of propagation of the excitations and the final charge transport, a special way of local periodic perturbations including appropriate phase shifts between neighboring units is proposed.

Radial models are used to investigate the processes of transfer and localization of the mechanical energy of radial displacements of DNA chains. As a critical amplitude is reached, these displacements lead to complete dissociation of a duplex into individual chains. Transfer and nonlinear packing of the energy of radial displacements of DNA chains cause many effects observed experimentally. Among them is an abrupt character of transverse micromechanical denaturation [19,20]. Other examples are a great heterogeneity of equilibrium constants for the heterogeneous duplex local opening, shown in experiments on promoter DNA fragments [14,15] and molecular beacons, studied by FCS method [21]: see also analysis of experiments performed in reference [10]. In this paper we shall show that in DNA containing excess charges, such as electrons and holes (cation-radicals) the transfer of the

[a] e-mail: mgvelarde@pluri.ucm.es

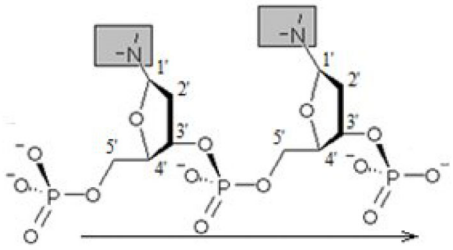

**Fig. 1.** Structure of a single DNA chain illustrating arrangement of its sugar-phosphate backbone and chains' direction.

mechanical energy of radial displacements of DNA chains is accompanied by the transfer of the excess charges along the molecule axis. This may be used in construction of DNA-based devices.

In Section 2 we schematically present the DNA structure and illustrate peculiarities of the description of its dynamics associated with different degrees of freedom of the bases in the models considered. For clarity we also describe in detail experimental evidence of the influence of energy transfer and localization in the duplex on its stability. The aim of this section is to substantiate the choice of the model relying on the experimental material accumulated thus far. In Section 3 we recall the *Peyrard-Bishop-Dauxois-Holstein* Hamiltonian model [22] and derive the dimensionless differential equations for the motion of the sites of a nucleotide chain and Schrödinger equation for the components of a discrete wave function of an electron interacting with the chain. There we also substantiate the choice of boundary and initial conditions for the dynamical regimes analyzed in the paper. In Section 4 we present the results of investigation of nonlinear oscillations and waves in DNA provoked by a short pulse excitation of the particle velocity and their interaction with an added excess charge. In Section 5 the results of similar investigations are given for the case of exciting the chain by a harmonic external excitation of the particles' velocities. The interaction of a polaron with breathers in DNA is considered in Section 6. A summary results found is given in Section 7.

## 2 Theoretical and experimental basis of the model chosen

A polymer DNA chain consists of a sugar-phosphate backbone joining up nitrogenous bases – adenine, guanine, cytosine and thymine. The backbone structure is shown in Figure 1: grey rectangles contain atoms N of nitrogenous bases joined by a glycosidic linkage with N-1' atom of the furanose ring. The segment consisting of deoxyribose, phosphate residue and a nitrogenous base is called a nucleotide.

Figure 1 also shows the directions of DNA chains – from the 5'-end to the 3'-end. The sequence of nucleotides in these directions is called a primary structure. The chains form a duplex in which adenine is held together with thymine by two H-bonds and guanine with cytosine –

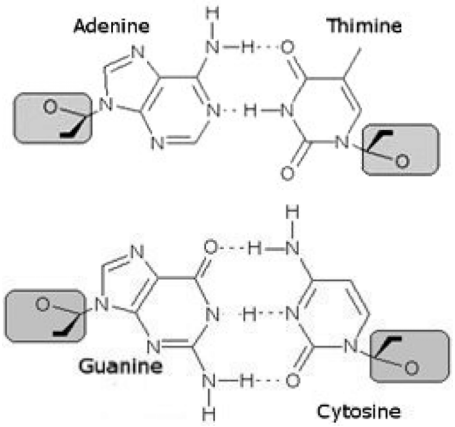


**Fig. 2.** Scheme of complementary interaction in DNA base pairs. Complementary H-bonds are shown in dashed lines. Here the arrow indicating the chain's direction in Figure 1 is perpendicular to the plane of the figure.

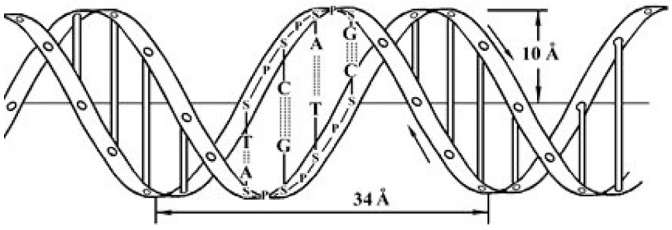


**Fig. 3.** Schematic representation of the structure of a DNA duplex.

by three H-bonds. This type of parallel bonding is called complementary while the basic bonding – a complementarity. The structure of bases and their complementary interaction are shown in Figure 2. The fragments of deoxyribose residue are shown in grey rectangles.

The chains of the duplex are joined in antiparallel and form a right-handed helix. The DNA geometry, its diameter and the size of a turn are shown in Figure 3. Letters S stand for deoxyribose residues and letters P – for phosphates. In radial models the degree of freedom is lengthening of the bundle of complementary H-bonds shown in Figures 2 and 3 by dashed lines.

The bases of one chain of a duplex reside in nearly parallel planes and are joined with one another by specific non-covalent bonds. Since the bases in such a structure resemble a stack of coins their arrangement in a single chain is often called a stack, while the bonds supporting the structure – stacking interactions.

Overlapping of $\pi$-orbitals in a stack leads to partial delocalization of $\pi$-electrons of nitrogenous heterocycles [23,24]. Since a stack is a $\pi$-conjugated system, cation-radicals can migrate in a duplex [25]. It plays an important role both in repairing DNA damages [26–28] and in the processes of carcinogenesis [29,30] and mutagenesis [16,29,31].

Apart from the influence on the charge transfer, a local transient duplex unwinding plays a major role, for example, in facilitating the DNA twisting when it is

packed into nucleosomes [32,33] or else in formation of ring molecules [32,34,35]. Even more important field of investigation is the study of interaction of different DNA open states with enzymes. In particular, it was experimentally proved that flip-out of bases from Watson-Crick helix is primary in promoter recognition in duplex DNA [3,4]. For the case of the radial duplex openings this question is controversial since experimental proofs of the key role of DNA dynamics in this case are less direct [14,15].

There is considerable experimental evidence testifying the fact that the strength of H-bonds and stacking interaction is by no means the only factor determining the kinetics of the local transient duplex openings. A great contribution into destabilization of the double helix is made by the processes of transfer and localization of the energy of nonlinear excitations of the duplex chains. The first evidence of the contribution of these processes was obtained in experiments on micromechanical DNA unzipping by stretching the complementary chains at one of its ends. In this case H-bonds break successively while the chains remain undamaged. In experiments by Bockelmann et al. mechanical unzipping of a homogeneous DNA occurred step-wise and involved some pronounced "stick-slip cycles" [19,36]. On a scale of several tens of base pairs the "force *versus* displacement" curves correlated well with the relation of adenine-thymine and cytosine nucleotide pairs' concentrations. However as the technology of optical tweezers was used which improved the resolution to the scale of tens of base pairs and even less, experimentalists faced with a considerable influence of non-equilibrium processes on the duplex resistance [20].

Subsequently sharp fluctuations of the mechanical resistance and its dependence on the rate of micromechanical unzipping were described with the use of a modified simple radial Peyrard-Bishop-Dauxois (PBD) model [37,38]. The authors showed a simple mechanism of arising fluctuations of DNA mechanical resistance upon unzipping. Due to non-uniform localization of the chain oscillation energy in DNA there are always short-living "opened" regions. Little energy if any is required for their unzipping, therefore mechanical resistance of the duplex in these regions sharply decreases until the front separating native DNA and its unzipped part again runs into a "closed" region where H-bonds are undamaged. This mechanism illustrates an important fact: "stick-slip cycles'" could be observed even in unzipping of a homopolymer DNA [37]. In other words, the energy transfer and localization are independent of whether DNA is homogeneous or heterogeneous.

Nevertheless, the effect of the energy transfer and localization is more pronounced in the open states' dynamics in a heterogeneous DNA. In 2004 Choi et al. tried to prove the antecedence of open states' dynamics in DNA-enzyme interactions and obtained rather unexpected results [14]. Using biochemical methods, the authors measured relative probability of the open states' emerging in different regions of some heterogeneous DNA. It turned out that the difference of equilibrium constants for duplex opening can be as large as two orders of magnitude and greater [14,15]. Moreover, replacement of just two adjacent base pairs at one point (instead of a wild type promoter a mutant one was taken) brought about a considerably increased stability in this point, but substantially decreased stability in the region separated from it by a distance of tens of nucleotide pairs.

The only approach which enabled one to reproduce these effects at least in part was Langevin dynamics in the already mentioned PBD model [14,15]. Some attempts to quicken calculations by passing on to investigation of equilibrium properties of PBD model actually led to a loss of agreement with experimental data [39–42]. In these papers the ratio between the minimum and maximum equilibrium constants in the duplex opening reaction did not exceed 0.15; the "long-range effect" of mutation was not observed either. The same situation occurred in passing on to simplified Langevin approach in which computing time was reduced due to the substantially increased friction coefficient [43].

Another important proof of the fact that the processes of energy transfer and localization have an effect on the DNA dynamics is the anomalously low stability of the so-called molecular beacons, thoroughly investigated in reference [21]. Analysis of these experiments is presented in detail in Sections 4.3 and 5.3 of review [10], therefore we will not dwell upon this problem here. Briefly speaking, in addition to many worthy experimental facts, the authors of reference [21] incidentally obtained indirect evidence for localization of the energy of nonlinear breathers in bent DNA regions. This effect was first predicted in PBD model seven years earlier [44]. The contribution of this mechanism into the duplex destabilization is described in Section 5.3.3 of paper [10].

The experimental facts cited above suggest that one of the main requirements for the DNA mechanical model is taking into account the energy localization which leads to the onset of high-amplitude nonlinear excitations. In great detail this problem is considered in reference [10]. This is successfully realized in PBD model. Therefore investigations of the model and its various modifications hold a prominent place among many works devoted to theoretical study of the duplex dynamics [45–52].

## 3 Peyrard-Bishop-Dauxois-Holstein model

Following the above cited arguments we will investigate the properties of the charge transfer in DNA in the framework of quantum-classical model which is a combination of Peyrard-Bishop-Dauxois [53] and Holstein models [54]. Instead of a simple description of the dynamics of excitations arising in a chain of nucleotide pairs (carried out in Holstein model) we use a more complete model suggested in reference [53]. The model is known as Peyrard-Bishop-Holstein model [22].

The interaction of the complementary nucleotides in Watson-Crick pair is called the "on-site" interaction. To describe this interaction we use a nonlinear Morse potential. The sites belonging to one helix are considered to be

units of a quasi-one-dimensional chain bound by nonlinear forces (stacking interactions). The stacking potential in the case of very small and very large deviations of the sites from the equilibrium position being nearly parabolic, though with different values of the elastic constant [55]. The Hamiltonian of the model in this case can be presented as

$$\hat{H} = \sum_{n}^{N} \alpha_n |n\rangle\langle n| + \sum_{n,m}^{N} v_{nm} |n\rangle\langle m| + \chi \sum_{n} (w_n - v_n) |n\rangle\langle n| + \sum_{n} \left\{ \frac{1}{2} m \left(\dot{w}_n^2 + \dot{v}_n^2\right) + \frac{\kappa}{2} \left[ (w_n - w_{n-1})^2 \left(1 + \rho e^{-\eta(w_n + w_{n-1})}\right) + (v_n - v_{n-1})^2 \left(1 + \rho e^{\eta(v_n + v_{n-1})}\right) \right] + U(w_n - v_n) \right\}, \quad (1)$$

where $\alpha_n$ is the charge energy at the $n$th site, $v_{nm}$ are coefficients of "hopping" integrals, $\chi$ is a charge-vibration coupling constant, $w_n, v_n$ are displacements of individual nucleotides in the $n$th nucleotide pair from the equilibrium position, $m$ is the nucleotide mass. Dot stands for the time derivatives of $w_n$ and $v_n$. The quantity $U(w_n - v_n)$ involved in (1) determines interaction of nucleotides in a pair. The middle term in the brackets in (1) is responsible for the interaction between neighboring nucleotides (stacking interaction). Its parameters are an elasticity coefficient $\kappa$ and correction coefficients $\rho$ and $\eta$ determining nonlinear deviation of stacking-potential from parabolic form in the case of intermediate values of nucleotide displacements.

If we seek a solution corresponding to Hamiltonian (1), in the form

$$|\Psi\rangle = \sum_{n} c_n(t) |n\rangle, \quad (2)$$

and introduce new variables

$$x_n = \frac{w_n + v_n}{\sqrt{2}}, \; y_n = \frac{w_n - v_n}{\sqrt{2}}, \quad (3)$$

then, the equations for the motion of nucleotide pairs and discrete Schrödinger equation for a charge, an electron and a hole, neglecting small values $x_n$ (in view of symmetry of the motion of nucleotides in the pair $w_n \approx v_{-n}$), may be written as:

$$m\frac{d^2 y_n}{dt^2} + \frac{\partial}{\partial y_n} \sum_{n} \left\{ \frac{\kappa}{2} \left[ (y_n - y_{n-1})^2 \left(1 + \rho e^{-\eta(y_n + y_{n-1})}\right) + (y_{n+1} - y_n)^2 \left(1 + \rho e^{-\eta(y_{n+1} + y_n)}\right) \right] + U(y_n) \right\} + \sqrt{2}\chi |c_n|^2 = 0, \quad (4)$$

$$i\hbar \frac{dc_n}{dt} = \alpha_n c_n + \sum_{m} v_{nm} c_m + \sqrt{2}\chi y_n c_n. \quad (5)$$

Therefore por Poly-G/Poly-C homogeneous chain in the nearest neighbor approximation we get ($\alpha_n \equiv 0$)

$$i\hbar \frac{dc_n}{dt} = -v(c_{n+1} + c_{n-1}) + \sqrt{2}\chi y_n c_n. \quad (6)$$

Assuming that the on-site potential in nucleotide pair can be approximated by the Morse potential [37,38,53]

$$U(y_n) = D\left(e^{-2\sigma y_n} - 2e^{-\sigma y_n}\right), \quad (7)$$

we obtain

$$\frac{d^2 q_n}{dt^2} = e^{-q_n}\left(e^{-q_n} - 1\right) + \omega_{bond}^2 \times \left[(q_{n+1} - 2q_n + q_{n-1}) + \rho f(q_{n-1,n,n+1})\right] - \chi_h |c_n|^2, \quad (8)$$

$$\frac{dc_n}{dt} = -i\tau_e (c_{n+1} + c_{n-1}) - i\chi_{el} q_n c_n, \quad (9)$$

$$f(q_{n-1,n,n+1}) = (q_{n-1} - q_n) e^{-\eta'(q_n + q_{n-1})} \times \left[1 - 2\eta'(q_n - q_{n-1})\right] + (q_{n+1} - q_n) e^{-\eta'(q_n + q_{n+1})} \times \left[1 - 2\eta'(q_{n+1} - q_n)\right]. \quad (10)$$

Here the elasticity coefficient $\sigma$ characterizes the bond stiffness, $q_n = \sigma y_n$ is a normalized displacement, $\tau = \omega_M t$ is dimensionless time, $\omega_M$ is the frequency of linear oscillations in an individual site ($\omega_M^2 = 2\sigma^2 D/m$), $\omega_{bond} = \left(\kappa/2\sigma^2 D\right)^{1/2}$ is the frequency of oscillations of sites in a chain normalized to $\omega_M$, $\chi_h = \sqrt{2}\chi/2\sigma D$ and $\chi_{el} = \sqrt{2}\chi/\hbar\omega_M\sigma = \chi_h (2D/\hbar\omega_M)$ are dimensionless parameters of bonding between the electron and the lattice, $\tau_e = \nu/\hbar\omega_M$ is a dimensionless parameter determining the ratio between the characteristic times of the evolution of an electron wave function and the dynamics of excitations in a lattice, $\hbar$ is Planck constant, function $f(q_{n-1,n,n+1})$ characterizes the nonlinear part of the bonding force between the sites, $\eta' = \eta/\sqrt{2}$.

In linear approximation for $\chi_h = 0$ and $\rho = 0$ it follows from (10) the equation

$$\frac{d^2 q_n}{dt^2} = -q_n + \omega_{bond}^2 \left[(q_{n+1} - 2q_n + q_{n-1})\right], \quad (11)$$

and the dispersion relation

$$\omega^2 = 1 + 4\omega_{bond}^2 \sin^2(k/2). \quad (12)$$

The latter suggests that the phonon spectrum is in the range of the frequencies between 1 and $\sqrt{1 + 4\omega_{bond}^2}$. Here $k$ is a dimensionless wave number on the scale determined by the distance between neighboring sites along the chain axis.

The equations (8)–(10) with specific initial conditions (see below) and periodic boundary conditions were solved numerically by using a fourth-order Runge-Kutta algorithm. The required accuracy is provided, in particular, by keeping constant the values of the system integrals. The integration step was chosen to be 0.001 or 0.0005, the number of sites $N = 50$–$200$, the characteristic times of simulations $10^2$–$10^3$. The values of dimensionless parameters were chosen in view of known estimates of geometrical and energetic characteristics of DNA molecule: $D = 0.04$ eV, $\sigma = 4.45$ Å$^{-1}$, $\kappa = 0.06$ eV/Å$^2$, $m = 300$ a.m.u. [56],

$v = 0.084$ eV (for Poly-G/Poly-C chain) [57], $\chi = 0.13$ eV/Å [57,58], $\rho = 0.5$, $\eta = 0.35$ Å$^{-1}$ [53]. It follows that $\omega_{bond} \approx 0.2$, $\tau_e = \nu/\hbar\omega_M \approx 18$, $\chi_h \approx 0.5$, $\chi_{el} \approx 8.5$.

The values of parameters used in numerical modeling were chosen with due regard to the assessments made. The peculiarity of this investigation is the way of exciting oscillations and waves in the chain via perturbation of the velocity of one or several neighboring sites by a strong external local action of duration rather short. As a result nonlinear localized local waves should arise in the chain. These waves will be able to trap an electron and localize it in position or transfer it along the chain without the need of an external electric field. Notice that excitation of a lattice due to initial *displacements* of the particles from equilibrium positions were considered, for example, in reference [59]. It was shown that formation of nonlinear localized waves in the form of breathers is possible. We will consider initial excitation of the *velocities* of DNA particles, i.e. assume that initial kinetic energy is introduced in the system.

## 4 Nonlinear oscillations and waves in DNA excited by short kick of one particle and through their interaction with the external charge

Let us assume that at the initial instant of time $\tau = 0$ a particle with number $n_{in}$ gets a strong kick and its velocity takes a value $v_0 \geq 1$ (the dimensionless velocity $v_0 = 1$ corresponds to the dimensionless energy of complementary H-bonds in an isolated nucleotide pair). At the same time a charged added excess particle (hereafter for brevity sake, an electron) gets on this particle. The wave function of the external particle is determined in the form of a narrow Gaussian pulse. Depending on the value of the initial pulse either a pinned breather with frequency $\omega_{br} < 1$ (Fig. 4., $v_0 = 1$, $\omega_{br} \approx 0.7$, and Fig. 5, $v_0 = 3$, $\omega_{br} \approx 0.45$), arises in the chain or a bubble with fronts symmetrically moving in opposite directions. Each front can be considered as a narrow mobile breather (Fig. 6, $v_0 = 16$, see also [58]). In this case, the components of the spectrum of the initial pulse, belonging to the phonon spectrum scatter in the lattice. The evolutions of the electron wave functions are different in all the three cases. If the breather is not very strong (with relatively small displacements and velocities of the particles), the initially localized electron quickly delocalizes itself (Figs. 4b and 4c) for any value of the coupling parameter $\chi_h$. The reason is that for small values of the parameter the breather cannot hold the electron, while for large ones the electron breaks the breather due to polaron effect – the electron tries to form a polaron in which the structure of the particles displacements does not correspond to the structure of displacements of the particles in the breather. However, a more powerful breather (Fig. 5, $v_0 = 3$) can trap the electron and form a pinned bound state "breather-electron" in a narrow range of the coupling parameter values ($\chi_{el} = 6$). To specify this state the term "breather-polaron" can also be used

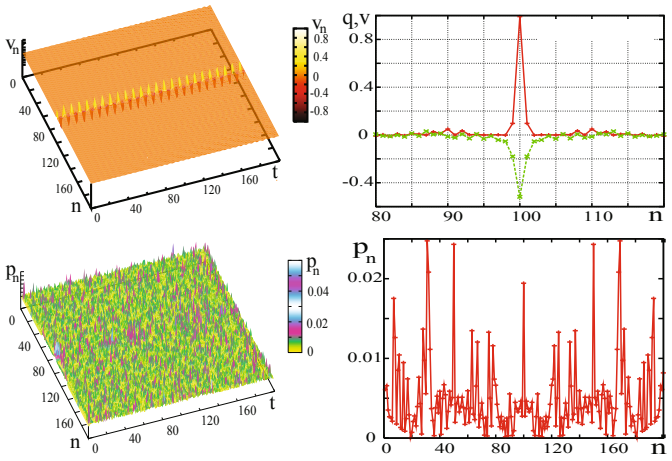


**Fig. 4.** Excitation of a pinned breather by initial kick of one particle ($v_0 = 1$, $n_{in} = 100$, $N = 200$, $\omega_{bond} \approx 0.2$) and delocalization of an electron ($\tau_e = 18$, $\chi_h = 0.5$, $\chi_{el} = 6$). The figure (upper level (a, c); lower level (b, d)) shows: (a) the time evolution of the distribution of particles velocities; (b) the distribution of the probability density, $p_n = |c_n|^2$, to find an electron in the chain; (c) distribution of displacements $q_n$ (red) and velocities $v_n$ (green) of particles; and (d) distribution of the probability density along the chain at the last moment of simulation for $t = 200$.

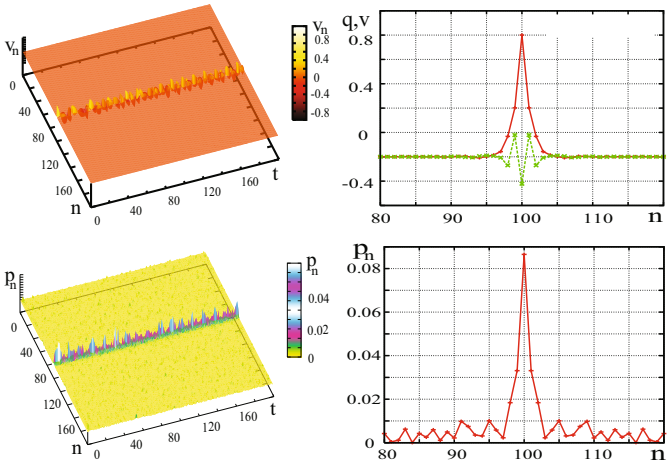


**Fig. 5.** Excitation of a pinned breather by initial kick of one particle ($v_0 = 3$, $n_{in} = 100$, $N = 200$, $\omega_{bond} \approx 0.2$) and trapping of an electron ($\tau_e = 18$, $\chi_h = 0.3$, $\chi_{el} = 6$). The figure (upper level (a, c); lower level (b, d)) shows: (a) the time evolution of the distribution of particles velocities; (b) the distribution of the probability density, $p_n = |c_n|^2$, to find an electron in the chain; (c) distribution of displacements $q_n$ (red) and velocities $v_n$ (green) of particles; and (d) distribution of the probability density along the chain (fragment $n = 80$–$120$) at the last moment of simulation for $t = 200$.

(polaro-breather [60]). But for the electron to transfer, the initial energy of excitation should be still higher. In this case a symmetrically expanding bubble is formed whose fronts have the structures of mobile breathers (Fig. 6, $v_0 = 16$). These breathers trap the electron, the probability of trapping by the "left" and "right" breathers is the same in view of symmetry. Therefore the electron wave

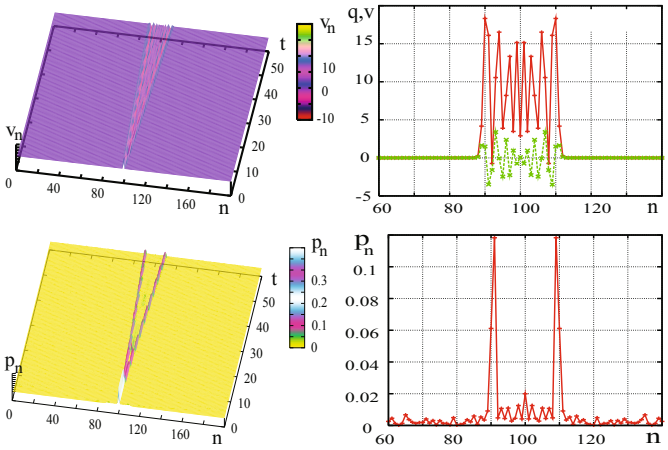


**Fig. 6.** Excitation of a bubble and breathers by a very strong (high momentum) initial pulse of one particle ($v_0 = 16$, $n_{in} = 100$, $N = 200$, $\omega_{bond} \approx 0.2$) and trapping and transfer of an electron ($\tau_e = 18$, $\chi_h = 0.5$, $\chi_{el} = 6$). The figure (upper level (a, c); lower level (b, d)) shows: (a) the time evolution of the distribution of particles velocities; (b) the distribution of the probability density, $p_n = |c_n|^2$, to find an electron in the chain; (c) distribution of displacements $q_n$ (red) and velocities $v_n$ (green) of particles; and (d) distribution of the probability density along the chain (fragment $n = 60$–$140$) at the last moment of simulation for $t = 60$.

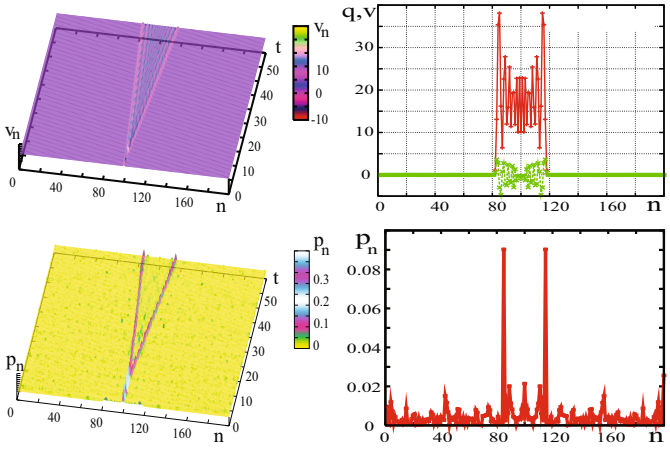


**Fig. 7.** Excitation of a bubble and breathers by harmonic disturbance of the velocity of one particle ($v_{in} = 0.0025$, $\omega_{in} \approx 0.7$, $\tau_{in} = 10$, $n_{in} = 100$, $N = 200$, $\omega_{bond} \approx 0.2$) and trapping and transfer of an electron ($\tau_e = 18$, $\chi_h = 0.5$, $\chi_{el} = 6$). The figure (upper level (a, c); lower level (b, d)) shows: (a) the time evolution of the distribution of particles velocities; (b) the distribution of the probability density, $p_n = |c_n|^2$, to find an electron in the chain; (c) distribution of displacements $q_n$ (red) and velocities $v_n$ (green) of particles; and (d) distribution of the probability density along the chain at the last moment of simulation for $t = 100$.

function or better said its probability density splits. This can happen if the distance between the localized states is not very large so that for the characteristic time of the electron transfer between these states, the chain's structure does not change considerably. In the case under consideration this condition can be assumed to be fulfilled since in the localized state "polaron-breather" the maximum displacement of the electron from its initial position is not very large, of the order of ten sites; besides it occurs during $\Delta\tau \sim 60$, where from one can assess the transfer rate, also the velocity of the breather $v_{br} \approx 0.15$, if we assume that the longitudinal coordinate (along the chain axis) is normalized to the value of the distance between the nucleotide pairs. Then the bubble stops expanding, breathers slow down, weaken and loose the electron which quickly delocalizes.

## 5 Nonlinear oscillations and waves in DNA excited by a periodic disturbance of the velocity of one or few particles in the chain

Another effective way to excite localized oscillations and waves is altering of the velocity of one or several particles by an external periodic force with the frequency of the order of that of a breather which, according to estimates, falls into Terahertz range [56]. We should have in mind that we need for such excitations very fine instruments like field emission microscopes with very small radius of action and very small intensities. Any local manipulation of the velocities should go through corresponding forces. This is very difficult but should be in the range of modern instruments at least in near future of developing nano mechanotronics. In this case there is a possibility to vary the values of the amplitude and pumping frequency, the duration of its action, the number of excited elements and the difference of oscillation phases between the oscillators.

Here first we will assume that the velocity of one particle (again with number $n_{in}$) initially changes harmonically ($v_n = v_{in} \sin(\omega_{in} t)$) during rather a short time interval $t_{in}$ of the order of a period of this function. The frequency $\omega_{in}$ is chosen to be less than 1 (i.e. less than the lower frequency of the phonon spectrum band), so that the external force be, on the average, in resonance with the oscillator frequency which decreases as the energy grows, while the value of $v_{in}$ is taken to be rather large so that the lattice would be able to get a lot of energy during a short time internal. As a result, again, depending on the values of the parameters $v_{in}$, $\omega_{in}$, $t_{in}$ localized structures similar to the above described ones are excited. Figure 7 presents the process of formation of an expanding bubble with fronts in the form of moving breathers which trap the electron initially located on the particle whose velocity is excited by the external harmonic force. On the whole the effect observed corresponds to the results presented above in Figure 6, however the electron transport is more effective here – the maximum displacement is more than half larger, the life-time of a bound state is also half as much, i.e. the transfer rate is virtually the same.

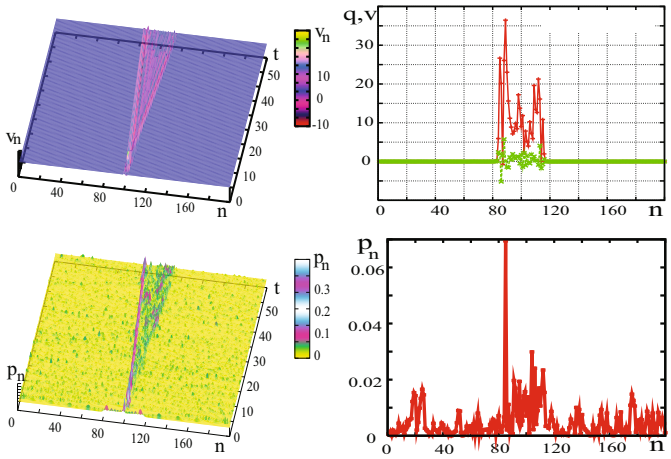


**Fig. 8.** Excitation of an asymmetric bubble and breathers by harmonic excitation of the velocity of four neighboring particles ($v_{in} = 0.0014$, $\omega_{in} \approx 0.72$, $\tau_{in} = 10$, $n_{in} = 100$–$103$, $\Delta\varphi_{in} = 1.4$, $N = 200$, $\omega_{bond} \approx 0.2$) and trapping and transfer of an electron ($\tau_e = 18$, $\chi_h = 0.5$, $\chi_{el} = 6$). The figure (upper level (a, c); lower level (b, d)) shows: (a) the time evolution of the distribution of particles velocities; (b) the distribution of the probability density, $p_n = |c_n|^2$, to find an electron in the chain; (c) distribution of displacements $q_n$ (red) and velocities $v_n$ (green) of particles; and (d) distribution of the probability density along the chain at the last moment of simulation for $t = 100$.

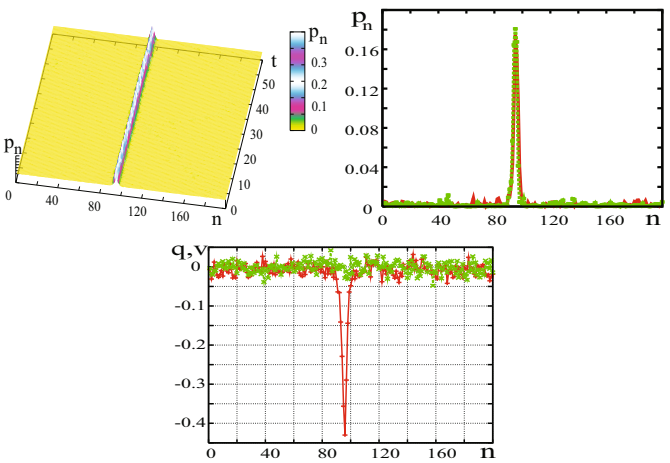


**Fig. 9.** Polaron in DNA.4.3 Time evolution, $t = 0$–$200$, of the state reached after a long transient process. The parameter values for $t = 200$ are used subsequently as initial conditions in modeling the polaron-breather interaction ($N = 200$, $\omega_{bond} \approx 0.2$, $\tau_e = 18$, $\chi_h = 4$, $\chi_{el} = 48$). The figure (in clockwise run: (a, b, c)) shows: (a) the time evolution of the distribution of the probability density, $p_n = |c_n|^2$, to find an electron in the chain; (b) distribution of the probability density for $t = 0$ (red) and $t = 200$ (green); and (c) distribution of displacements $q_n$ (red) and velocities $v_n$ (green) of particles for $t = 200$ along the chain.

The peculiarity of this way of excitation is the possibility to determine the preferred direction of the charge transfer if we realize excitation of several neighboring particles with appropriate phase shift of harmonic influence of the same frequency. A typical result of such approach is presented in Figure 8. In this case four particles were excited and the phase shift of the exciting force $\Delta\varphi$ was 1.4. Therefore the excitation waves running to the left interfere nearly in phase, while those running to the right-out of phase. As a result, the amplitude of the wave running to the left turns out to be nearly twice as high as the amplitude of the wave running to the right. If we choose $\Delta\varphi = -1.4$, the wave running to the right will prevail. By such way we provide a preferred direction of the electron transport in the direction of propagation of the prevailing wave. The parameters of such asymmetric transport are nearly the same as those in the case of "symmetric" transport.

In conclusion it should be mentioned that by varying the parameters in the range of admissible values we can try to find a set of values for which the life-time of the bound state will be maximal. It can also be thought that the difference of the excitation phases can be realized not only between neighboring sites but also between groups of sites (clusters) inside which particles oscillate in phase. Notice that the study of the dynamics of DNA affected by an external force is of independent interest which, in particular, is stimulated by development of terahertz technologies [61].

## 6 Interaction of a polaron and a breather in DNA

Another mechanism of electron transport caused by nonlinear excitations in the chain arises when a polaron is formed in a DNA molecule and subsequently a breather is excited in one of the above-described ways. The question arises: is a controllable transport of a polaron due to its interaction with the breather possible? The steady polaron state of an electron in DNA is thoroughly studied and the possibility of its existence in the system under consideration is practically ensured (see, for example [62–70] and references therein). Notice, however that in studying the evolution of the polaron state it should be born in mind that the characteristic times of the evolution depend on the values of the interaction parameter $\chi_h$. In particular, when the parameter value $\chi_h = 0.5$ is used, the evolution times are very large, therefore in the numerical experiment the polaron was formed from the initial localized electron state in the form of a Gaussian pulse in the course of a long transition process with a large value of the interaction parameters $\chi_h = 4$, $\chi_{el} = 48$ and considerable friction coefficient providing attenuation of phonons arising in the process of polaron formation ("cooling" of the lattice). As a result, a state was obtained in which the main excitation energy is concentrated in the polaron and only a small portion of the total energy belongs to small excitations outside the polaron (Fig. 9). The sites of the polaron oscillate only weakly and their displacements from the equilibrium position are negative. This means that around the polaron tapering occurs in contrast to a breather where, in view of asymmetry of the Morse potential, positive values

of the displacement prevail (compare Figs. 5c–6c; 7c–8c, and 9c). Therefore, we can hardly expect, for example, that a polaron and a breather may merge. However the polaron formed should respond to changes in the chain structure since the electron energy tends to reach the minimum value. On the other hand, since the electron in the polaron is bound to the lattice, the lattice's structure should rearrange in the polaron region which requires some energy. Accordingly, the polaron though resistant to small excitations, it should respond to large ones. These assumptions are fully confirmed by the results of numerical simulations.

Indeed, it was found that the polaron once formed is not significantly deformed in the case of a small initial excitation of the velocity of one particle $|v_0| \leq 1$, even if the particle being excited dislocates in close proximity to the polaron. However if we increase the value of $|v_0|$, we can notice that for rather a large value of the initial excitation energy, the polaron starts traveling trying to move away from the arising breather. Figures 10a–10c, ($v_0 = 1$) demonstrate that a polaron which centers initially at $n = n_{pol} = 96$, uniformly shifts to the distance of $n = 5$ from its initial position during the time $t = 100$. It is due to the influence of the breather, excited by a kick to the particle with number $n = 105$ and taking the velocity $v_0 = 1$. The velocity of the displacement is $v_{pol} = 0.05$. Then the polaron virtually stops (for $t > 100$).

If the breather energy increases, the polaron velocity and the value of displacement grow (Figs. 10d–10f, $v_0 = 2$), and for $v_0 \geq 5$, when the expanding bubble is excited they become very large (Figs. 10g–10i, $v_0 = 8$), i.e. larger than in the cases considered above. However the transformation of the evolution patterns of the wave function distribution (while the energy of the initial excitation is increasing) is not monotonic, distributions of the kind of those presented in Figures 10a and 10g, can intersperse with the evolution patterns presented in Figure 10d. This is probably concerned with the relation of the phases of the wave functions of the electron and phonons accompanying excitation of the breather. The consequence is also a non-monotonic dependence of the polaron velocity on the initial excitation energy. Nevertheless, the analysis suggests that, on the average, the velocity of a polaron induced by a breather grows along the curve shown in Figure 11.

Displacement of a polaron can be larger than that presented in Figure 10, however in the course of time the polaron can slow down, deform itself, and fade away. Therefore, for definiteness, we have considered a limited (though long) time interval $t = 200$, during which the polaron motion can be considered to be nearly uniform and be characterized by a mean value of the velocity and, accordingly, current.

## 7 Concluding remarks and summary of results found

Understanding effective charge transfer in DNA-like molecular wires is of paramount importance for the development of nanobioelectronics [8,9,71]. Traditionally,

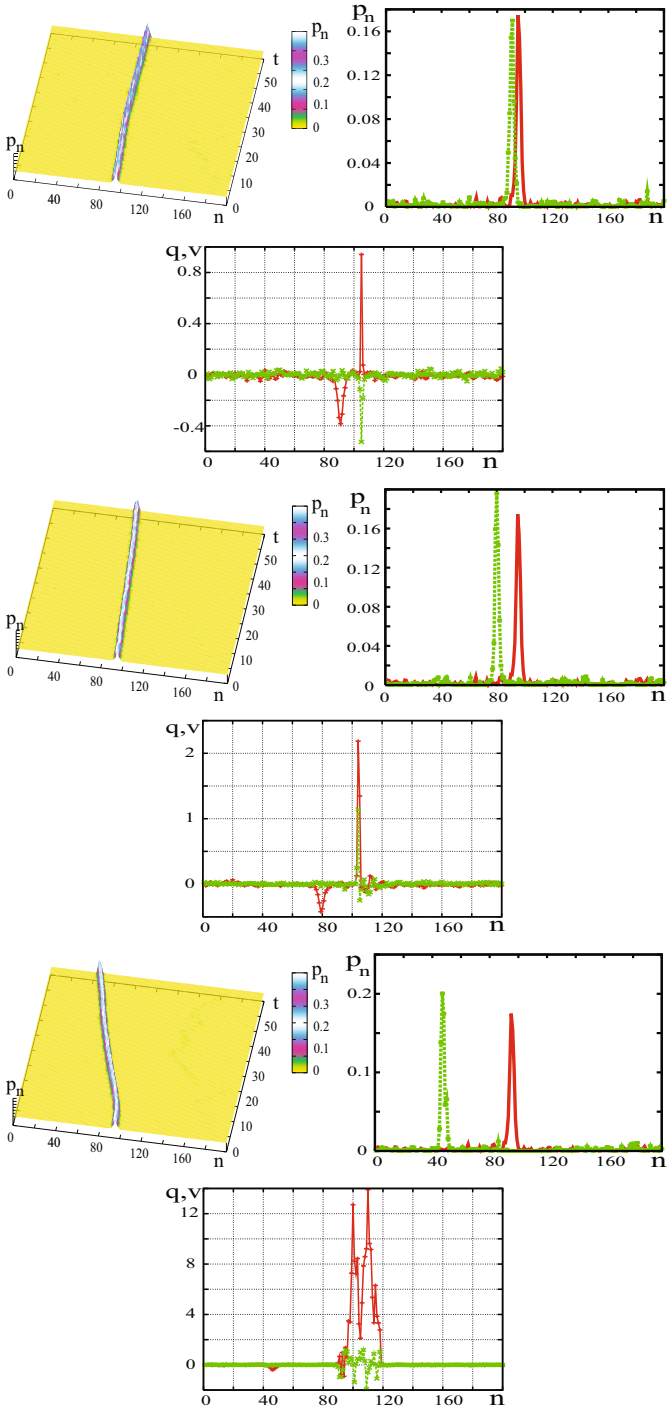


**Fig. 10.** Interaction of a polaron with a breather in DNA. Initially the polaron is centered at site $n = 96$, the breather is excited by the initial kick of a particle at site $n = 105$. The figure (by blocks of the three panels reading in clockwise run; (a, b, c); (d, e, f); (g, h, i)) shows the time evolution of the distribution of the probability density, $p_n = |c_n|^2$, to find an electron in the chain (a, d, g); distribution of the probability density for $t = 0$ (red) and $t = 200$ (green) (b, e, h); distribution of displacements $q_n$ (red) and velocities $v_n$ (green) of particles for $t = 200$ (c, f, i) along the chain. For the top row $v_n = 1$, for the middle row $v_n = 2$, for the bottom row $v_n = 8$. $N = 200$, $\omega_{bond} \approx 0.2$, $\tau_e = 18$, $\chi_h = 4$, $\chi_{el} = 48$.

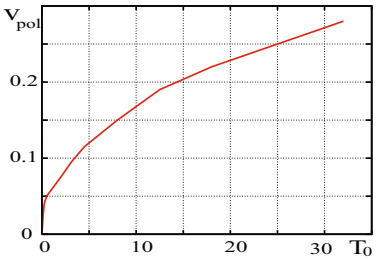


**Fig. 11.** Approximate dependence of the polaron velocity $v_{pol}$ on the energy of the initial pulse $v_{in}^2/2$ for the case presented in Figure 10. $N = 200$, $\omega_{bond} \approx 0.2$, $\tau_e = 18$, $\chi_h = 4$, $\chi_{el} = 48$.

by the force responsible for the charge transfer is meant the potential difference induced between the nanowire ends. According to [65,66], theoretical estimates of the charge mobility in DNA yield a small value of this quantity: $\mu \sim 1 \times 10^{-4}$ cm$^2$/V s. Thus it is known that in a "dry" chain the value of the hole mobility $\mu$ is of the order of 1 cm$^2$/V s [67–69]. For "wet" chains, i.e. chains in a solution, where a great role belongs to solvation effects, the mobility turns out to be several orders of magnitude lower than for "dry" ones [65,66]. The use of DNA-wires with so low mobility makes them to be of little promise for nanobioelectronics purposes.

The results obtained in this paper offer the alternative charge transfer via nonlinear localized excitations as carriers which exist in DNA even in the absence of charges introduced there. Earlier this possibility was suggested for model nonlinear molecular chains in references [72–74].

In this paper we investigated the interaction of excess charges inserted in DNA with nonlinear DNA excitations in the framework of *Peyrard-Bishop-Dauxois-Holstein* model [22,53,54]. Our main results are:

(1) In the framework of *Peyrard-Bishop-Dauxois-Holstein* model, we have carried out numerical modeling of the interaction of an external charged particle (electron or hole) with nonlinear localized oscillations and waves in DNA excited via an external excitation of the velocity of one or several particles (a short kick providing momentum rather than space displacement).
(2) We have shown that upon a local strong enough excitation of the DNA lattice, breathers can arise on the moving fronts of a bubble formed due to the nonlinear nature of the bubble lattice. These breathers can trap an added, excess external electron and transfer it along the chain. The characteristic time of the existence of the "breather-electron" bound state is of the order of 20–30 periods of the lattice's sites oscillations. The characteristic displacement length is ∼20 sites. The maximum probability to find an electron in the moving breather is ∼0.2.
(3) We have also shown that if the lattice contains a motionless polaron and then a breather (though not very powerful) is excited, then, as a result of the polaron-breather interaction, the polaron tends to travel at a rather high velocity, moving away from the breather. The characteristic length of the trajectory, i.e. the distance over which the charge is transferred, can be very large ∼100–200 sites. The velocity of the traveling polaron grows, on the average, as the breather energy increases. One can expect that this mechanism brings the possibility to control the characteristics of the charge transport in DNA-like wires.

For experimental realization of the described phenomena, one can use atomic scanning probe microscope, whose tip is brought to the DNA molecule and injects there a charge which leads to local heating of the molecule and formation of a soliton, a breather, or a bubble in the place of injection, as is described in references [75,76]. It can also be assumed that the tip of the scanning probe microscope can provoke localized excitations, solitons and breathers by a short impulse or a set of impulses at one end of DNA, and these formations, while traveling along the molecule can trap polarons or stimulate their motion, providing their transport along DNA. Thus we propose here a special method of external local perturbations. This method allow to control the direction of propagation of polarons, and their charge transport. Our method includes appropriate phase shifts between the excitation of neighbors.

The considered effect of excitation of breathers-bubbles by the periodic action on a local spot in a DNA fragment requires a source of high-frequency oscillations $\omega \sim 10^{12}$ s$^{-1}$, including a spatial resolution at the nanoscale and time resolution at picosecond scale. At present such a problem is not solved yet, since in real force microscopes the maximum frequency does not exceed $10^5$–$10^6$ Hz [61], however, the ongoing development of terahertz technologies offers hope.

The work was done with the support from the RFBR, Project No. 16-07-00305 and from the Russian Ministry of Education and Science (Project No. 1008).

## References

1. J. Cerny, P. Hobza, Phys. Chem. Chem. Phys. **9**, 5291 (2007)
2. C.J. Benham, S.P. Mielke, Ann. Rev. Biomed. Eng. **7**, 21 (2005)
3. A. Feklistov, S.A. Darst, Cell **147**, 1257 (2011)
4. X. Liu, D.A. Bushnell, R.D. Kornberg, Cell **147**, 1218 (2011)
5. L.V. Yakushevich, *Nonlinear Physics of DNA*, 2nd edn. (Wiley-VCH, Weinheim, 2004)
6. G.B. Schuster, in *Long-range Charge Transfer in DNA* (Springer, Berlin, 2004), Vol. 2
7. B. Giese, Acc. Chem. Res. **33**, 631 (2000)
8. V.D. Lakhno, J. Quant. Chem. **108**, 1970 (2008)
9. G.P. Triberis, M. Dimakogianni, Recent Patents on Nanotechnology **3**, 135 (2009)
10. A.S. Shigaev, O.A. Ponomarev, V.D. Lakhno, Mathematical Biology & Bioinformatics **8**, 553 (2013) (in Russian)
11. J. Marmur, P. Doty, J. Mol. Biol. **5**, 109 (1962)
12. R.B. Inman, R.L. Baldwin, J. Mol. Biol. **8**, 452 (1964)
13. E. Folta-Stogniew, I.M. Russu, Biochem. **33**, 11016 (1994)

14. C.H. Choi, G. Kalosakas, K.O. Rasmussen, M. Hiromura, A.R. Bishop, A. Usheva, Nucl. Acids Res. **32**, 1584 (2004)
15. G. Kalosakas, K.O. Rasmussen, A.R. Bishop, C.H. Choi, A. Usheva, Europhys. Lett. **68**, 127 (2004)
16. H.-A. Wagenknecht, Nat. Prod. Rep. **23**, 973 (2006)
17. K.Ø Rasmussen, A.R. Bishop, Phys. Rev. B **68**, 174304 (2003)
18. G. Kalosakas, K. Rasmussen, A.R. Bishop, Synth. Metals **141**, 93 (2004)
19. U. Bockelmann, B. Essevaz-Roulet, F. Heslot, Phys. Rev. Lett. **79**, 4489 (1997)
20. U. Bockelmann, Ph. Thomen, B. Essevaz-Roulet, V. Viasnoff, F. Heslot, Biophys. J. **82**, 1537 (2002)
21. G. Altan-Bonnet, A. Libchaber, O. Krichevsky, Phys. Rev. Lett. **90**, 138101 (2003)
22. S. Komineas, G. Kalosakas, A.R. Bishop, Phys. Rev. E **65**, 061905 (2002)
23. A.K. Tewari, R. Dubey, Bioorg. Med. Chem. **16**, 126 (2008)
24. F. Gago, Methods **14**, 277 (1998)
25. D.D. Eley, D.I. Spivey, Trans. Faraday Soc. **58**, 411 (1962)
26. J.C. Genereux, A.K. Boal, J.K. Barton, J. Am. Chem. Soc. **132**, 891 (2010)
27. P.A. Sontz, T.P. Mui, J.O. Fuss, J.A. Tainer, J.K. Barton, Proc. Natl. Acad. Sci. USA **109**, 1856 (2012)
28. P.A. Sontz, N.B. Muren, J.K. Barton, Accounts Chem. Res. **45**, 1792 (2012)
29. B. Armitage, Chem. Rev. **98**, 1171 (1998)
30. S. Kawanishi, Y. Hiraku, S. Oikawa, Mutation Res. **488**, 65 (2001)
31. K. Kino, H. Sugiyama, Chem. Biol. **8**, 369 (2001)
32. T. Cloutier, J. Widom, Mol. Cell. **14**, 355 (2004)
33. J. Yan, J.F. Marko, Phys. Rev. Lett. **93**, 108108 (2004)
34. T. Cloutier, J. Widom, Proc. Natl. Acad. Sci. USA **102**, 3645 (2005)
35. Q. Du, C. Smith, N. Shiffeldrim, M. Vologodskaia, A. Vologodskii, Proc. Natl. Acad. Sci. USA **102**, 5397 (2005)
36. B. Essevaz-Roulet, U. Bockelmann, F. Heslot, Proc. Natl. Acad. Sci. USA **94**, 11935 (1997)
37. M. Peyrard, Europhys. Lett. **44**, 271 (1998)
38. M. Peyrard, Nonlinearity **17**, R1 (2004)
39. T.S. van Erp, S. Cuesta-Lopez, M. Peyrard, Eur. Phys. J. E **20**, 421 (2006)
40. Z. Rapti, A. Smerzi, K.O. Rasmussen, A.R. Bishop, C.H. Choi, Europhys. Lett. **74**, 540 (2006)
41. Z. Rapti, A. Smerzi, K.O. Rasmussen, A.R. Bishop, Phys. Rev. E **73**, 051902 (2006)
42. C.H. Choi, Z. Rapti, V. Gelev, M.R. Hacker, B. Alexandrov, J.S. Park, E.J. Park, N. Horikoshi, A. Smerzi, K.O. Rasmussen, A.R. Bishop, A. Usheva, Biophys. J. **95**, 597 (2008)
43. F. de los Santos, O. Al Hammal, M.A. Munoz, Phys. Rev. E **77**, 032901 (2008)
44. J.J.-L. Ting, M. Peyrard, Phys. Rev. E **53**, 1011 (1996)
45. C.B. Tabi, A. Mohamadou, T.C. Kofane, Phys. Scr. **77**, 045002 (2008)
46. C.B. Tabi, A. Mohamadou, T.C. Kofane, Eur. Phys. J. B **74**, 151 (2010)
47. P. Maniadis, B.S. Alexandrov, A.R. Bishop, K.O. Rasmussen, Phys. Rev. E **83**, 011904 (2011)
48. S. Zhravkovic, M.V. Sataric, Phys. Scr. **64**, 612 (2001)
49. S. Zdravkovic, M.V. Sataric, Phys. Rev. E **77**, 031906 (2008)
50. J. Cuevas, J.F.R. Archilla, Yu.B. Gaididei, F.R. Romero, Physica D **163**, 106 (2002)
51. P.V. Larsen, P.L. Christiansen, O. Bang, J.F.R. Archilla, Yu.B. Gaididei, Phys. Rev. E **69**, 026603 (2004)
52. A. Alvarez, F.R. Romero, J.F.R. Archilla, J. Cuevas, P.V. Larsen, Eur. Phys. J. B **51**, 119 (2006)
53. T. Dauxois, M. Peyrard, A.R. Bishop, Phys. Rev. E **47**, R44 (1993)
54. T. Holstein, Ann. Phys. **8**, 325 (1959)
55. M. Peyrard, S. Cuesta-Lopez, G. James, Nonlinearity **21**, 91 (2008)
56. T. Dauxois, M. Peyrard, A.R. Bishop, Phys. Rev. E **47**, 684 (1993)
57. A.S. Shigaev, O.A. Ponomarev, V.D. Lakhno, Chem. Phys. Lett. **513**, 276 (2011)
58. V.D. Lakhno, A.P. Chetverikov, Mathematical Biology & Bioinformatics **9**, 4 (2014) (in Russian)
59. E. Zamora-Sillero, A.V. Shapovalov, F.J. Esteban, Phys. Rev. E **76**, 066603 (2007)
60. J. Cuevas, P.G. Kevrekidis, D.J. Frantzeskakis, A.R. Bishop, Phys. Rev. B **74**, 064304 (2002)
61. P.H. Siegel, IEEE Trans. Microwave Theory Techniques **50**, 910 (2002)
62. B.S. Alexandrov, V. Gelev, A.R. Bishop, A. Usheva, K.O. Rasmussen, Phys. Lett. A **374**, 1214 (2010)
63. G. Kalosakas, K.O. Rasmussen, A.R. Bishop, J. Chem. Phys. **118**, 3731 (2003)
64. G. Kalosakas, Phys. Rev. E **84**, 051905 (2011)
65. D.M. Basko, E.M. Conwell, Phys. Rev. Lett. **88**, 098102 (2002)
66. V.D. Lakhno, N.S. Fialko, Zh. Fiz. Khim. **86**, 832 (2012)
67. F. Grozema, L.D.A. Siebellis, Y.A. Berlin, M. Ratner, ChemPhysChem **3**, 536 (2002)
68. V.D. Lakhno, N.S. Fialko, J. Exp. Theor. Phys. Lett. **78**, 336 (2003)
69. V.D. Lakhno, N.S. Fialko, Eur. Phys. J. B **43**, 279 (2005)
70. V.D. Lakhno, A.N. Korshunova, Mathematical Biology & Bioinformatics **5**, 1 (2010) (in Russian)
71. *Nanobioelectronics for Electronics Biology and Medicine*, edited by A. Offenhausser, R. Rinald (Springer, New York, 2009)
72. M.G. Velarde, W. Ebeling, A.P. Chetverikov, Int. J. Bifurc. Chaos **15**, 245 (2005)
73. M.G. Velarde, W. Ebeling, D. Hennig, C. Neissner, Int. J. Bifurc. Chaos **16**, 1035 (2006)
74. M.G. Velarde, J. Computat. Appl. Math. **233**, 1432 (2010)
75. H.W. Fink, C. Schonenberger, Nature **398**, 407 (1999)
76. F. Giessibl, Rev. Mod. Phys. **75**, 949 (2003)